Aberrant Visual-Related Networks in Familial Cortical Myoclonic Tremor with Epilepsy

Haotian Wang
Zhejiang University School of Medicine Second Affiliated Hospital https://orcid.org/0000-0002-7677-8930

Bo Wang
Zhejiang University School of Medicine Second Affiliated Hospital

Zhidong Cen
Zhejiang University School of Medicine Second Affiliated Hospital

Jue Wang
Chengdu Sport University

Yu-Feng Zang
Hangzhou Normal University

Dehao Yang
Zhejiang University School of Medicine Second Affiliated Hospital

Yao Ding
Zhejiang University School of Medicine Second Affiliated Hospital

Shuang Wang
Zhejiang University School of Medicine Second Affiliated Hospital

Sheng Wu
Zhejiang University School of Medicine Second Affiliated Hospital

Wei Luo (luoweirock@zju.edu.cn)
Zhejiang University School of Medicine Second Affiliated Hospital

---

Research Article

Keywords: familial cortical myoclonic tremor with epilepsy, regional homogeneity, degree centrality, primary visual cortex, photoparoxysmal response.

Posted Date: September 27th, 2021

DOI: https://doi.org/10.21203/rs.3.rs-910998/v1

Abstract

In familial cortical myoclonic tremor with epilepsy, photic stimulation can trigger visual-related symptoms and induce a photoparoxysmal response on electroencephalography. This is known as photosensitivity. To explore the mechanism of prominent visual-related symptoms and photosensitivity in patients with genetically confirmed familial cortical myoclonic tremor with epilepsy type 1, resting-state functional magnetic resonance imaging data and electroencephalography data were collected from 31 patients carrying the heterozygous pathogenic intronic pentanucleotide (TTTCA)n insertion in the sterile alpha motif domain-containing 12 gene and from 52 age- and sex-matched healthy controls. Results: (1) Both regional homogeneity and degree centrality values in the bilateral calcarine sulcus were significantly increased in patients compared with HCs. (2) When the calcarine sulcus area with increased regional homogeneity was taken as a seed, increased functional connectivity values were observed in the right precentral gyrus, while decreased functional connectivity values were observed in the right superior frontal gyrus and right inferior parietal lobule. (3) independent component analysis showed increased connectivity in the left calcarine sulcus inside the medial visual network. (4) Correlation analysis revealed significant positive correlation between regional homogeneity values and frequency of seizure, and photoparoxysmal response grades were positively correlated with the severity of cortical tremor and duration of epilepsy. The findings provide strong evidence for the interpretation of visual-related symptoms and photosensitivity in familial cortical myoclonic tremor with epilepsy and may also relate to other epilepsy syndromes with photosensitivity. We speculate the significant functional change in primary visual cortex probably an imaging biomarker for the disease.

Significance Statement:

Photic stimulation induced apparent visual-related symptoms and a high prevalence of photosensitivity in FCMTE. Wang et al.'s findings provide strong evidence to explain the visual-related symptoms and photosensitivity.

Introduction

Familial cortical myoclonic tremor with epilepsy (FCMTE) is a rare autosomal dominant epilepsy syndrome with genetic and clinical heterogeneity. It is also known as benign adult familial myoclonic epilepsy in Japan or autosomal-dominant cortical myoclonus and epilepsy or familial adult myoclonic epilepsy in Europe.[1,2] Expanded intronic pentanucleotide (TTTCA)n insertion in the sterile alpha motif domain-containing 12 gene (*SAMD12*) is the genetic cause of FCMTE1 in Japanese,[3] Chinese,[4] Sri Lankan and Indian populations.[5] Similar mutations have been identified in five other genes (*STARD7*, *MARCH6*, *YEAST2*, *TNRC6A* and *RAPGEF2*) in FCMTE2–4, 6 and 7, respectively. The two major clinical features of cortical tremor, which is characterized by tremulous involuntary movements in distal upper extremities, and infrequent epilepsy attack are well recognized. In addition to the two major symptoms,

other symptoms, such as visual intolerance,[6] night blindness, and migraine, are also reported in FCMTE patients.

Photic stimulation may play an important role in FCMTE. It has been wildly reported that photic stimulation can exaggerate cortical tremor and precipitate epileptic attack.[1,7] Patients can also present visual intolerance, with patients unable to tolerate changes to ambient light or prolonged exposure to TV and computer screens or video games. Furthermore, intolerance to light always occurs in the second and third decades of life in patients already having cortical tremor and is considered a marker of disease progression. Photic stimulation-induced myoclonus has also been reported.[8] On EEG, intermittent photic stimulation (IPS) can trigger a photoparoxysmal response (PPR), also known photosensitivity, with prevalence ranging from 24.5 to 95% in FCMTE.[7,9,10] Photosensitivity is a hallmark of photosensitive epilepsy, including FCMTE, juvenile myoclonic epilepsy, idiopathic occipital photosensitive epilepsy, et al., and is strongly influenced by genetic factors.[11,12] Therefore, study of the mechanism of photosensitivity can help reveal the pathogenesis of FCMTE and also of other photosensitivity epilepsies. Considering the prominent clinical and EEG features of FCMTE in response to photic stimulation, we hypothesized the existence of abnormal local neural activities in visual regions that probably involve visual-related networks in patients at resting state.

Resting-state functional magnetic resonance imaging (RS-fMRI) studies have provided some understanding of FCMTE. Previous MRI studies have shown structural, functional and metabolic changes in the cerebellum by diffuse tensor imaging,[13] voxel-based morphometry of MRI images[14] and proton magnetic resonance spectroscopy.[15] MRI studies have also shown impaired brain activity in cortical areas[16] and altered cerebellar-cerebral functional connectivity (FC).[17] However, the above neuroimaging findings cannot explain the visual symptoms and photosensitivity. We recently conducted a RS-fMRI study in patients with genetically confirmed heterozygous FCMTE1 and observed an altered cerebello-motor network.[18] We did not find abnormalities in visual-related regions, probably because of strict multiple testing correction and the high threshold we set for percent amplitude fluctuation.

Regional homogeneity (ReHo) and seed-based FC can assess synchronization of both local and distant brain activity.[19] Degree centrality (DC) can determine the strength of the connectivity of one voxel compared with all other voxels in the brain.[20] Independent component analysis (ICA), a data-driven approach, is widely used for the analysis of functional networks in fMRI data and can effectively determine the functional characteristics of mutually correlated brain components.[21] The purpose of the current study was to investigate differences in intrinsic regional brain activity between genetically confirmed FCMTE1 patients and HCs using indices of ReHo and DC based on RS-fMRI, and to apply seed-based FC to evaluate aberrant distant networks. Furthermore, considering the prominent visual symptoms and photosensitivity in FCMTE, we measured the ICA-derived visual networks. Our results support our hypothesis and provide complementary insights into the established pathophysiological hypothesis of FCMTE.

Methods

Participants

Thirty-one patients with FCMTE1, the same population examined in our previous MRI study,[18] and 52 healthy controls (HCs) were enrolled. The inclusion and exclusion criteria for both groups were described previously.[18] All participants were right-handed, native Chinese. Detailed clinical data were collected by two neurologists. The Fahn-Tolosa-Marin Tremor Rating Scale (FTMRS) was used to assess the severity of cortical tremor in patients. EEG recording was performed on 29 patients. IPS was performed using a standard procedure in accordance with the updated European algorithm for visual stimulation. Three technicians and one neurologist reviewed and analyzed the EEG data. This study was approved by the ethics committee of the Second Affiliated Hospital, Zhejiang University School of Medicine and by the ethics committee of the Center for Cognition and Brain Disorders at the Affiliated Hospital of Hangzhou Normal University. Written informed consent was obtained from all participants prior to the study.

Head motion was estimated by mean framewise displacement based on the measures derived from Jenkinson's algorithm of relative root mean square. ReHo and DC metrics were sensitive to head motion. To control bias, we excluded participants with head motion surpassing 2 mm in any direction of translation or 2 degrees in any direction of rotation as well as mean framewise displacement exceeding one standard deviation (SD, 0.04 mm) above the sample mean (0.06 mm). These criteria excluded four patients and three HCs, leaving 27 patients and 49 HCs for further data analysis.

MRI Data Acquisition

MRI data were acquired with a 3-Tesla scanner (MR-750; GE Medical Systems, Milwaukee, WI) at the Center for Cognition and Brain Disorders, Affiliated Hospital of Hangzhou Normal University. MRI scanning sessions were as follows: (1) RS-fMRI (43 axial slices, repetition time [TR] = 2000 ms, echo time [TE] = 30 ms, flip angle = 90 degrees, field of view [FOV] = 220 × 220 mm, voxel size = 3.44 × 3.44 × 3.20 mm, 240 time points); (2) high-resolution T1-weighted image (176 sagittal slices, thickness = 1 mm, TR = 8.1 ms, TE = 3.1 ms, flip angle = 8 degrees, FOV = 256 × 256 mm).

MRI data Processing

Data pre-processing was conducted using DPARSF 5.1 (http://rfmri.org/dpabi)[22] and SPM12 (https://www.fil.ion.ucl.ac.uk/spm) based on MATLAB.

The preprocessing steps were as follows: (1) manual setting of the T1 images and functional images to the anterior commissure; (2) discarding the first 10 volumes of RS-fMRI data for signal equilibrium and participant adaptation to the scanning noise; (3) slice timing correction for the acquisition time delay between slices; (4) head motion correction; (5) co-registering individual T1 images to functional images; (6) removing the linear trend of the time courses; (7) regressing out nuisance signals including 24 head motion parameters, global mean, white matter, and cerebrospinal fluid signals; (8) spatial normalization to Montreal Neurological Institute (MNI) space by Diffeomorphic Anatomical Registration with the

Exponentiated Lie Algebra algorithm tool (DARTEL) (resample voxel size = 3 × 3 × 3mm); (9) applying a temporal filter with a bandpass of 0.01–0.1 Hz. Spatial smoothing was applied to FC with full width half maximum (FWHM) of 6 mm before band filter and FC calculation.

For the ReHo calculation, the Kendall concordance coefficient was calculated for the time courses of 27 neighboring voxels within a predefined gray matter mask (provided by SPM12, with tissue probability > 20%). For DC calculation, we applied a threshold to the correlation coefficients at $r > 0.25$ to remove weak correlations caused by noise, and negative connections were excluded when calculating binarized DC maps because of their ambiguous interpretation. The predefined gray matter mask above was used to restrict the DC calculation within the gray matter. ReHo and DC maps were then spatially smoothed with FWHM 6 mm. For the FC calculation, the peak T-value voxel of the brain area showing significant ReHo differences between FCMTE patients and HCs was selected as the seed (radius = 4 mm) to perform voxel-wise FC analysis within the gray matter mask. For every participant, ReHo, DC and FC maps were transformed to z-value maps using Fishers z-transformation.

For ICA analysis, RS-fMRI data was first preprocessed using DPARSF, including discarding the first 10 volumes, slice timing, head motion correction, normalizing by DARTEL and smoothing with FWHM of 6 mm. Group spatial ICA was performed using the Group ICA/IVA of the fMRI Toolbox (GIFT, https://trendscenter.org/software/gift/, version 3.0 c).[23] Processing steps were as follows: (1) remove mean per time point (2) the minimum description length was used to estimate the number of independent components, and 34 components were analyzed for each subject. (3) Data reduction used principal component analysis followed by independent component estimation to produce spatial maps and time courses with the infomax algorithm. To ensure the stability of independent component (IC) estimation, ICA was repeated 20 times in ICASSO.[24] (4) The IC time courses and the spatial maps of individual subjects were reverse reconstructed using GICA. (5) The mean ICA components were standardized into Z-scores across participants. (6) Three components of visual networks, including the lateral (or secondary) visual network, the medial (or primary) visual network, and the occipital visual network, were identified in accordance with a previous study.[25] (7) For each component, a one sample T test was used to create separate group-specific masks of patients and HCs (voxel level $p < 0.001$, cluster level $p < 0.05$, two-tailed), which were then combined into a total component mask.

Statistical analysis

The ReHo, DC and FC images were examined by independent t-tests performed in DPABI within the predefined gray matter mask described above. ICA images were examined within the component mask described above and the T maps were corrected using Gaussian random field (GRF) correction (voxel level $p < 0.001$, cluster level $p < 0.05$, two-tailed). The voxels above the threshold of ReHo, DC, FC and ICA were selected as regions of interest (ROIs) to extract the mean values for further analysis.

The mean values of ReHo, DC, FC and ICA, as well as clinical variables among participates were compared separately using SPSS 25.0 software (SPSS, Chicago, IL, USA), The relationships of fMRI indices and clinical variables (duration of cortical tremor, FTMRS score, duration of epilepsy, frequency of

seizures) and PPR grades, were detected using Spearman correlation and Pearson correlation. The relationships of PPR grades and clinical variables, were detected using Spearman correlation. $P < 0.05$ was considered to have statistical significance and Bonferroni correction was used to further determine the significance threshold for multiple measurements.

Results

Demographic information of FCMTE1 patients and HCs are shown in Supplementary Table S1. Independent t-tests and Pearson's chi-squared test were used to compare demographic differences between groups. There was no significant difference in age or sex between the two groups. All patients were confirmed to carry a heterozygous pathogenic $(TTTCA)_n$ insertion in *SAMD12*. All patients had cortical tremor while no apparent tremor in 52 HCs. Epileptic attack could be triggered by strong light or flicker in three patients, and visual intolerance was found in nine FCMTE1 patients.

Patients were divided into three subgroups according to the frequency of epileptic attack per year; six patients had no epileptic attack, 12 patients had less than one attack per year and 13 had one or more attack per year. EEG recording with IPS was performed on 28 patients. Twenty-four patients presented PPR on EEG, and when PPR was further graded on a scale from 1 to 4 according to Waltz[25] classification, six patients had PPR grade 2, five patients had PPR grade 3 and 13 patients had PPR grade 4. Fourteen patients received antiepileptic treatments (valproic acid: n = 9; oxcarbazepine, n = 1; carbamazepine, n = 1; clonazepam n = 3).

fMRI group differences

Group differences in independent t tests showed increased ReHo values in patients compared with HCs in the bilateral calcarine sulcus (corrected by GRF, voxel level $p < 0.001$, cluster level $p < 0.05$; Fig. 1 and Table 1). The results of DC were similar to those of ReHo but with more voxels above the threshold (Fig. 1 and Table 1).

Table 1
Brain regions showing significant differences between FCMTE patients and HCs

Indices	Brain Region	BA	Peak MNI coordinates			Peak T Value	Cluster Size (voxels)	Voxel Level P Value
			x	y	z			
ReHo	Calcarine sulcus (L)	17, 18	-9	-84	9	5.72	150	< 0.001
DC	Calcarine Sulcus (L)	17, 18	-12	-81	9	5.30	594	< 0.001
FC	Precentral gyrus (R)	6	30	-15	69	4.60	57	< 0.001
	superior frontal gyrus (R)	10	33	63	0	-5.11	100	< 0.001
	inferior parietal lobule (R)	40	48	-51	51	-4.46	62	< 0.001
ICA	Calcarine sulcus (L)	17	-9	-84	9	4.35	40	< 0.001

BA, Brodmann area; MNI, Montreal Neurological Institutes; L, Left hemisphere; R, Right hemisphere; ReHo, Regional homogeneity; DC, Degree centrality; FC, Functional connectivity; ICA, Independent component analysis.

Functional connectivity between the calcarine sulcus and the right precentral gyrus

The peak voxel of the brain area with increased ReHo in the calcarine sulcus was selected as a seed (x = -9, y = -84, z = 9, radius = 4 mm) to perform voxel-wise FC analysis. Increased FC values were observed in the right precentral gyrus, and decreased FC values were observed in the right superior frontal gyrus and right inferior parietal lobule in patients compared with HCs (GFR correction, voxel level $p < 0.001$, cluster level $p < 0.05$; Fig. 2 and Table 1).

Independent Component Analysis

Three component-related visual networks were selected that correspond to medial, occipital pole, and lateral visual networks (Supplementary Fig. 1). Group differences in independent t tests showed increased values in patients compared with HCs in the left calcarine sulcus in the medial visual network (corrected by GRF, voxel level $p < 0.001$, cluster level $p < 0.05$; Fig. 3 and Table 1).

Clinical correlations

Positive correlation was found between ReHo values and frequency levels of epilepsy (Spearman correlation, p = 0.028, r_s=0.422; Fig. 4A and Supplementary Table S2). There was no significant result between FC or DC values and clinic variables. FTMRS scores exhibited a significant positive correlation with PPR grade (Spearman correlation, p = 0.009, rs = 0.484; Fig. 4B and Supplementary Table S2). Duration of epilepsy exhibited positive correlation with PPR grade (Spearman correlation, p = 0.026, rs = 0.421; Fig. 4C and Supplementary Table S2).

Discussion

We found apparent visual-related symptoms in FCMTE1, such as epileptic attack triggered by strong light or flicker, visual intolerance. We recorded a high prevalence (87.5%) of PPR on EEG, also known as photosensitivity, and a high grade of PPR (grade 3 or 4) was presented by the majority of patients (75%). It is generally regarded that a high grade of PPR is prominently associated with epilepsy,[11] which was confirmed by our results. Furthermore, significant positive correlations were found between PPR grade and FTMRS scores and duration of epilepsy. Thus, we concluded that photosensitivity was not only an isolated EEG feature of FCMTE, but was also closely related to the two major symptoms. This might explain why photic stimulation can exaggerate cortical tremor and induce epileptic attacks.

Involvement of the primary visual cortex and primary visual network in FCMTE1

Compared with HCs, both increased ReHo and DC values were found in the bilateral calcarine sulcus in FCMTE1 patients. ICA analysis demonstrated increased connectivity between the left calcarine sulcus and the rest of the region inside the medial visual network (also known as the primary visual network) in the patient cohort. The calcarine sulcus is part of the primary visual cortex and receives visual information directly from visual stimulation. Studies using visual-evoked potentials or transcranial magnetic stimulation have shown intrinsic hyperexcitability in the visual cortex of patients with photosensitivity.[26,27] However, we found no correlation between PPR grades and MR indices. This may indicate that the damage in the primary visual cortex may be sufficient to produce a floor effect where gradation of severity is lost. This altered neural activity in the primary visual cortex and increased connectivity within the primary visual network in FCMTE1 patients probably contribute to the prominent visual-related symptoms and participate in the genesis of photosensitivity, suggesting a significant role of the central visual cortex in the pathophysiology of FCMTE and providing a potential imaging biomarker for the disease.

Altered visual-motor network in FCMTE1

We found increased FC between the primary visual cortex and the right precentral gyrus (BA 6) in the FCMTE1 patients. The increased FC between the primary visual cortex and the motor cortex can explain why the visual stimulation could induce or exaggerate the two major symptoms, cortical tremor and epileptic seizure. In addition, the ReHo values of the primary visual cortex were positively related to the

frequency of epilepsy. This means that the higher frequency of epilepsy the higher the ReHo values in the primary visual cortex, indicating that the aberrant visual-motor pathway may participate in the epileptic pathophysiology of FCMTE1. The established pathophysiological hypothesis posits that cortical hyperexcitability arising from cerebellar defects[1] explain the two major motor symptoms. The altered visual-motor network observed in the current study can complement the established hypothesis for the two motor symptoms.

In addition, this altered visual-motor network might also be associated with photosensitivity. Overactive visuomotor connections were found in patients with PPR in a transcranial magnetic stimulation study.[28] Studies using combined EEG-fMRI have shown increased neural activation within premotor and parietal cortex in addition to visual cortex in patients with photosensitivity after IPS-induced grade 4 PPR.[21] Network level changes were also found in patients with photosensitive epilepsy, that is abnormal activation of the striato-thalamo-cortical network with activation of the putamen and deactivation of motor related areas.[29] Taken together, we deduced this altered visual-motor network might also participate in the pathogenesis of photosensitivity in patients with FCMTE.

The aberrant dorsal visual pathway in FCMTE1

We also found decreased FC between the primary visual cortex and the right inferior parietal lobule and the right superior frontal gyrus in patients with FCMTE1. The inferior parietal lobule receives projections from the primary visual cortex, forming the dorsal visual pathway, which is probably relevant to spatial perception and codes visual information for action organization.[30,31] The dorsal visual pathway also has a predominant anatomical connection with the dorsal prefrontal cortex. In a working memory fMRI study, the superior frontal gyrus was considered selectively involved during working memory for shape.[32] Thus, we speculated that patients with FCMTE might have reduced transmission of visual information in the dorsal visual pathway. Further research on visual information processing in FCMTE is warranted.

Several limitations should be addressed in the current study. Firstly, synchronous EEG was not performed with the RS-fMRI and, therefore, we could not directly speculate on the epileptic and EEG traits in the current study. Secondly, some patients had taken antiepileptic drugs, which can confound results. Thirdly, our RS-fMRI findings are new for FCMTE and their neurophysiological relevance is not clear and need further experimental investigation.

Conclusion

In the past, the pathophysiological hypothesis of FCMTE mainly focused on the cerebellum and motor cortex. The current study provided a new perspective for understanding the disease and enriched the existing pathophysiological hypothesis. Photic stimulation induced apparent visual-related symptoms and a high prevalence of photosensitivity in FCMTE. Our findings of involvement of the primary visual cortex and the primary visual network, the aberrant distant visual-related networks, including the visual-motor network and the dorsal visual pathway, provide strong evidence to explain the visual-related

symptoms and photosensitivity. The significant functional change in primary visual cortex might be an imaging biomarker for the disease. They also as photosensitivity is the hallmark of photosensitivity epilepsy, e.g., juvenile myoclonic epilepsy, our findings are important for understanding the pathogenesis of other photosensitivity epilepsies. Meanwhile, the cortex and network involved in FCMTE might be candidate targets for intervention, for example using repetitive transcranial magnetic stimulation.

Declarations

Acknowledgements

We gratefully thank all participants for their invaluable collaboration, especially most of the patients who are from all over the country and need to take a long trip to participant in our study.

Funding: This study was supported by the Science Technology Department of Zhejiang Province (2019C03017) and the National Natural Science Foundation of China (No. 81520108016, No. 81571089 and No. 81371266).

Conflicts of interest/Competing interests: All authors claim that there are no conflicts of interest.

Ethics approval: This study was approved by the ethics committee of the Second Affiliated Hospital, Zhejiang University School of Medicine and by the ethics committee of the Center for Cognition and Brain Disorders at the Affiliated Hospital of Hangzhou Normal University.

Consent to participate: Written informed consent was obtained from all participants prior to the study.

Consent for publication: Not applicable

Availability of data and material: The data of PPR and FTMRS are available on request from the corresponding author. The data containing private information of participants are not publicly available (e.g., their mutation carriership).

Code availability: Not applicable

Authors' contributions: Author contributions included conception and study design (H.W., B.W., and Z.C.), data collection or acquisition (H.W., D.Y., Z.C., Y.D., S.Wang., S.Wu., and W.L.), statistical analysis (H.W., J.W., and Y.Z.), interpretation of results (H.W., B.W., Z.C., and J.W.), drafting the manuscript work or revising it critically for important intellectual content (H.W., B.W., Z.C., J.W., and W.L.) and approval of final version to be published and agreement to be accountable for the integrity and accuracy of all aspects of the work (All authors).

References

1. Van Den Ende, T., Sharifi, S., Van Der Salm, S. M. A., & Van Rootselaar, A. F. (2018). Familial cortical myoclonic tremor and epilepsy, an enigmatic disorder: From phenotypes to pathophysiology and genetics. A systematic review. *Tremor and Other Hyperkinetic Movements*. 8, doi:10.7916/D85155WJ
2. Cen, Z., Huang, C., Yin, H., et al. (2016). Clinical and neurophysiological features of familial cortical myoclonic tremor with epilepsy. *Mov Disord*, 31(11), 1704–1710. doi:10.1002/mds.26756
3. Florian, R. T., Kraft, F., Leitão, E., et al. (2019). Unstable TTTTA/TTTCA expansions in MARCH6 are associated with Familial Adult Myoclonic Epilepsy type 3. *Nat Commun*, 10(1), doi:10.1038/s41467-019-12763-9
4. Cen, Z., Jiang, Z., Chen, Y., et al. (2018). Intronic pentanucleotide TTTCA repeat insertion in the SAMD12 gene causes familial cortical myoclonic tremor with epilepsy type 1. *Brain*, 141(8), 2280–2288. doi:10.1093/brain/awy160
5. Bennett, M. F., Oliver, K. L., Regan, B. M., et al. (2020). Familial adult myoclonic epilepsy type 1 SAMD12 TTTCA repeat expansion arose 17,000 years ago and is present in Sri Lankan and Indian families. *Eur J Hum Genet*, 28(7), 973–978. doi:10.1038/s41431-020-0606-z
6. Magnin, E., Vidailhet, M., Ryff, I., Ferreira, S., Labauge, P., & Rumbach, L. (2012). Fronto-striatal dysfunction in type 3 familial cortical myoclonic tremor epilepsy occurring during aging. *J Neurol*, 259(12), 2714–2719. doi:10.1007/s00415-012-6575-6
7. Kobayashi, K., Hitomi, T., Matsumoto, R., Watanabe, M., Takahashi, R., & Ikeda, A. (2018). Nationwide survey in Japan endorsed diagnostic criteria of benign adult familial myoclonus epilepsy. *Seizure*, 61, 14–22. doi:10.1016/j.seizure.2018.07.014
8. Gardella, E., Tinuper, P., Marini, C., et al. (2006). Autosomal dominant early-onset cortical myoclonus, photic-induced myoclonus, and epilepsy in a large pedigree. *Epilepsia*, 47(10), 1643–1649. doi:10.1111/j.1528-1167.2006.00636.x
9. Binelli, S., Ragona, F., Canafoglia, L., et al. (2015). Electroencephalographic (EEG) Photoparoxysmal Responses under 5 Years of Age. *J Child Neurol*, 30(13), 1824–1830. doi:10.1177/0883073815583687
10. Toyota, T., Akamatsu, N., Tanaka, A., Tsuji, S., & Uozumi, T. (2014). Electroencephalographic features of benign adult familial myoclonic epilepsy. *Clin Neurophysiol*, 125(2), 250–254. doi:10.1016/j.clinph.2013.08.002
11. Padmanaban, V., Inati, S., Ksendzovsky, A., & Zaghloul, K. (2019). Clinical advances in photosensitive epilepsy. *Brain Res*, 1703, 18–25. doi:10.1016/j.brainres.2018.07.025
12. Poleon, S., & Szaflarski, J. P. (2017). Photosensitivity in generalized epilepsies. *Epilepsy Behav*, 68, 225–233. doi:10.1016/j.yebeh.2016.10.040
13. Buijink, A. W. G., Caan, M. W. A., Tijssen, M. A. J., Hoogduin, J. M., Maurits, N. M., & Van Rootselaar, A. F. (2013). Decreased cerebellar fiber density in cortical myoclonic tremor but not in essential tremor. *Cerebellum*, 12(2), 199–204. doi:10.1007/s12311-012-0414-2
14. Buijink, A. W. G., Broersma, M., van der Stouwe, A. M. M., et al. (2016). Cerebellar Atrophy in Cortical Myoclonic Tremor and Not in Hereditary Essential Tremor—a Voxel-Based Morphometry Study.

Cerebellum, 15(6), 696–704. doi:10.1007/s12311-015-0734-0

15. Long, L., Song, Y., Zhang, L., et al. (2015). A case-control proton magnetic resonance spectroscopy study confirms cerebellar dysfunction in benign adult familial myoclonic epilepsy. *Neuropsychiatr Dis Treat*, 11, 485–491. doi:10.2147/NDT.S77910
16. Wang, P., Luo, C., Dong, L., et al. (2015). Altered intrinsic brain activity in patients with familial cortical myoclonic tremor and epilepsy: An amplitude of low-frequency fluctuation study. *J Neurol Sci*, 351(1–2), 133–139. doi:10.1016/j.jns.2015.03.005
17. Long, L., Zeng, L. L., Song, Y., et al. (2016). Altered cerebellar-cerebral functional connectivity in benign adult familial myoclonic epilepsy. *Epilepsia*, 57(6), 941–948. doi:10.1111/epi.13372
18. Wang, B., Wang, J., Cen, Z., et al. (2020). Altered Cerebello-Motor Network in Familial Cortical Myoclonic Tremor With Epilepsy Type 1. *Mov Disord*, 35(6), 1012–1020. doi:10.1002/mds.28014
19. Zang, Y., Jiang, T., Lu, Y., He, Y., & Tian, L. (2004). Regional homogeneity approach to fMRI data analysis. *Neuroimage*, 22(1), 394–400. doi:10.1016/j.neuroimage.2003.12.030
20. Zuo, X. N., Xu, T., Jiang, L., et al. (2013). Toward reliable characterization of functional homogeneity in the human brain: Preprocessing, scan duration, imaging resolution and computational space. *Neuroimage*, 65, 374–386. doi:10.1016/j.neuroimage.2012.10.017
21. Zuo, X. N., Ehmke, R., Mennes, M., et al. (2012). Network centrality in the human functional connectome. *Cereb Cortex*, 22(8), 1862–1875. doi:10.1093/cercor/bhr269
22. Yan, C. G., Wang, X., Di, Zuo, X. N., & Zang, Y. F. (2016). DPABI: Data Processing & Analysis for (Resting-State). *Brain Imaging. Neuroinformatics*, 14(3), 339–351. doi:10.1007/s12021-016-9299-4
23. Calhoun, V. D., Adali, T., Pearlson, G. D., & Pekar, J. J. (2001). A method for making group inferences from functional MRI data using independent component analysis. *Hum Brain Mapp*, 14(3), 140–151. doi:10.1002/hbm.1048
24. Ma, S., Correa, N. M., Li, X. L., Eichele, T., Calhoun, V. D., & Adali, T. (2011). Automatic identification of functional clusters in fMRI data using spatial dependence. *IEEE Trans Biomed Eng*, 58(12 PART 1), 3406–3417. doi:10.1109/TBME.2011.2167149
25. Wang, Y., Lu, W., Xie, Y., et al. (2020). Functional Alterations in Resting-State Visual Networks in High-Tension Glaucoma: An Independent Component Analysis. *Front Hum Neurosci*. 14, doi:10.3389/fnhum.2020.00330
26. Strigaro, G., Prandi, P., Varrasi, C., Monaco, F., & Cantello, R. (2012). Defective visual inhibition in photosensitive idiopathic generalized epilepsy. *Epilepsia*, 53(4), 695–704. doi:10.1111/j.1528-1167.2012.03411.x
27. Suppa, A., & Rocchi, L. (2016). Visual cortex hyperexcitability contributes to the pathophysiology of the photoparoxysmal response. *Clin Neurophysiol*, 127(10), 3351–3352. doi:10.1016/j.clinph.2016.07.002
28. Strigaro, G., Falletta, L., Varrasi, C., Rothwell, J. C., & Cantello, R. (2015). Overactive visuomotor connections underlie the photoparoxysmal response. A TMS study. *Epilepsia*, 56(11), 1828–1835. doi:10.1111/epi.13190

29. Bartolini, E., Pesaresi, I., Fabbri, S., et al. (2014). Abnormal response to photic stimulation in Juvenile Myoclonic Epilepsy: An EEG-fMRI study. *Epilepsia*, 55(7), 1038–1047. doi:10.1111/epi.12634
30. Rizzolatti, G., & Matelli, M. (2003). Two different streams form the dorsal visual system: Anatomy and functions. *Experimental Brain Research*, Vol 153, 146–157. doi:10.1007/s00221-003-1588-0
31. Kravitz, D. J., Saleem, K. S., Baker, C. I., Ungerleider, L. G., & Mishkin, M. (2013). The ventral visual pathway: An expanded neural framework for the processing of object quality. *Trends Cogn Sci*, 17(1), 26–49. doi:10.1016/j.tics.2012.10.011
32. Yee, L. T. S., Roe, K., & Courtney, S. M. (2010). Selective involvement of superior frontal cortex during working memory for shapes. *J Neurophysiol*, 103(1), 557–563. doi:10.1152/jn.91299.2008

Figures

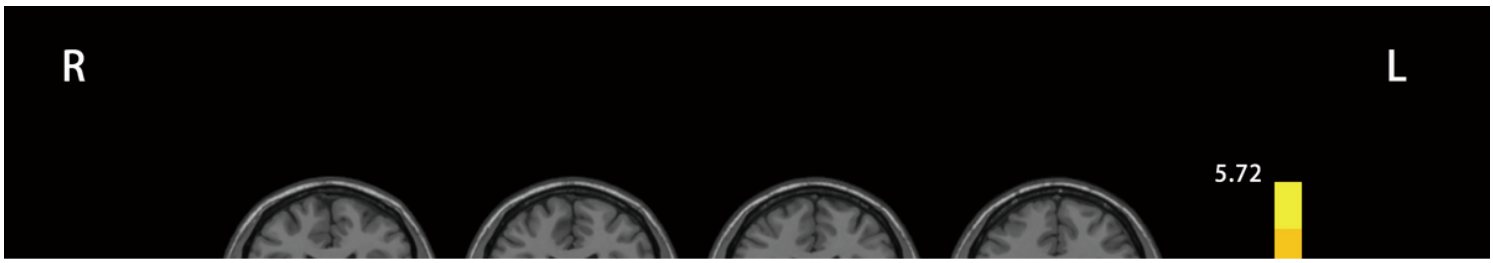

Figure 1

Increased ReHo in the bilateral calcarine sulcus (corrected by GRF, voxel level p<0.001, cluster level p<0.05). Increased DC in the bilateral calcarine sulcus (corrected by GRF, voxel level p<0.001, cluster level p<0.05).

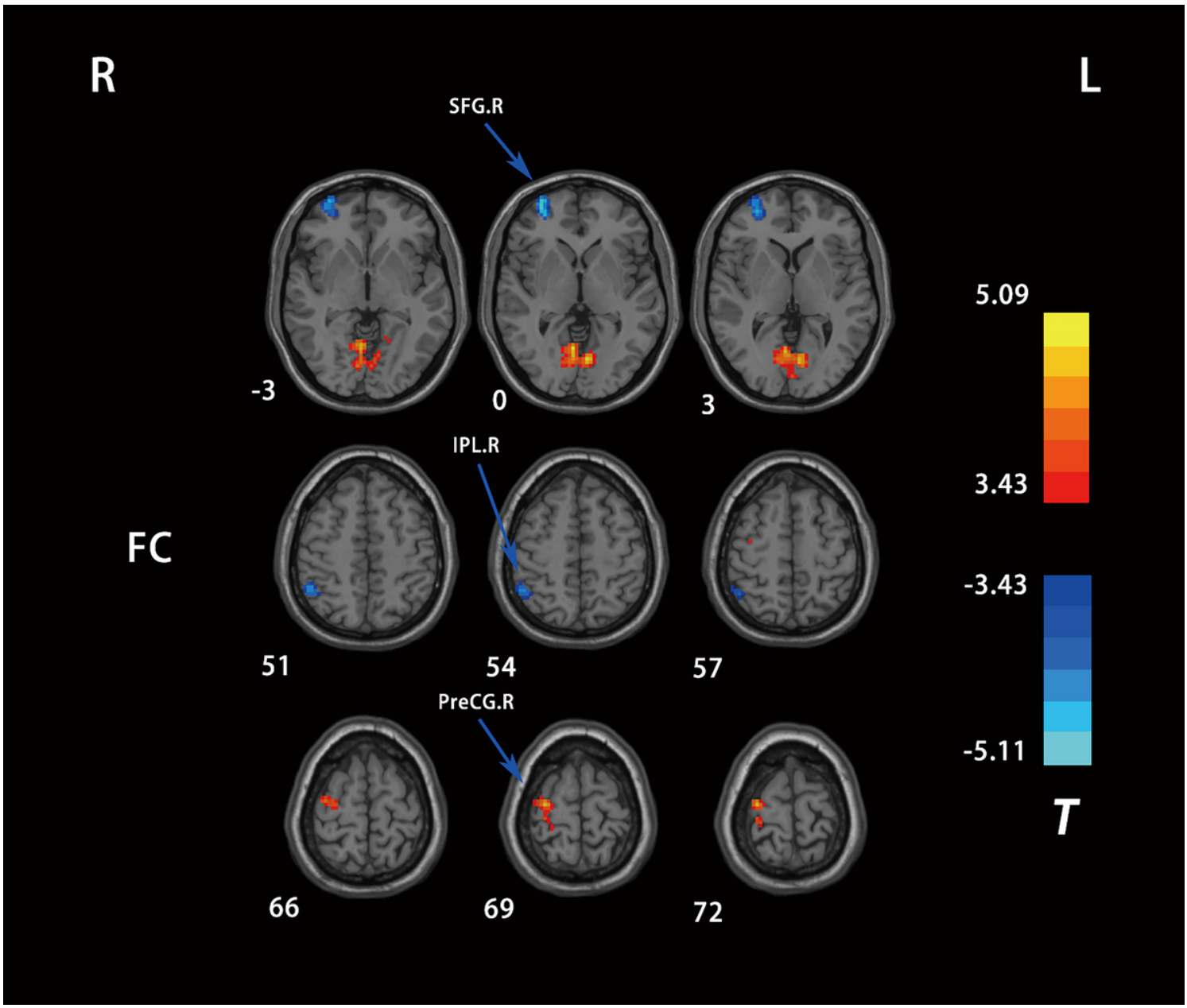

Figure 2

Increased FC in the right precentral gyrus. Decreased FC in the superior frontal gyrus and the inferior parietal lobule (corrected by GRF, voxel level p<0.001, cluster level p<0.05). SFG.R, right superior frontal gyrus; IPL.R, right inferior parietal lobule; PreCG.R, right precentral gyrus.

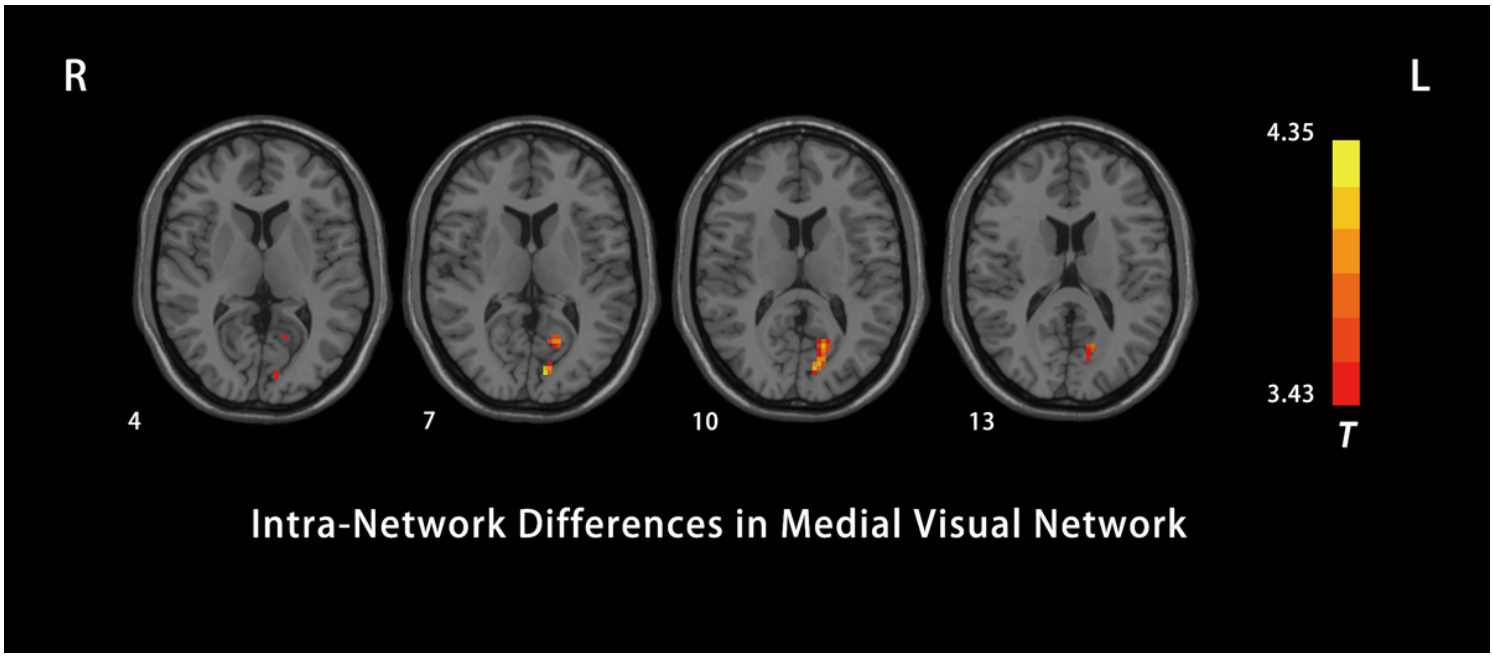

Figure 3

Increased strength of connectivity in patients compared with HCs in the left calcarine sulcus in the medial visual network.

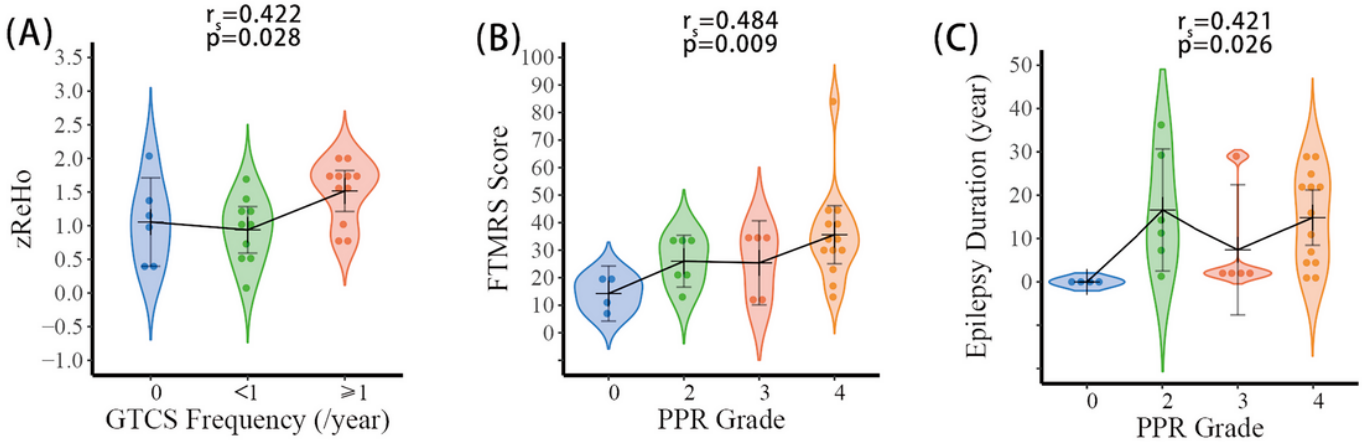

Figure 4

Spearman correlations between ReHo, DC and clinical assessments of patients. (A) ReHo against frequency of tonic-clonic seizures. (B) FTMRS scores against PPR grades. (C) Epilepsy duration against PPR grades.

Supplementary Files

This is a list of supplementary files associated with this preprint. Click to download.

- AuthorChecklist.pdf
- Fig.S1.tif
- TableS1.docx
- TableS2.docx